Cell Reports Methods, Volume *2*

Supplemental information

Deep-learning analysis of micropattern-based organoids enables high-throughput drug screening of Huntington's disease models

Jakob J. Metzger, Carlota Pereda, Arjun Adhikari, Tomomi Haremaki, Szilvia Galgoczi, Eric D. Siggia, Ali H. Brivanlou, and Fred Etoc

Figure S1 related to Figure 1

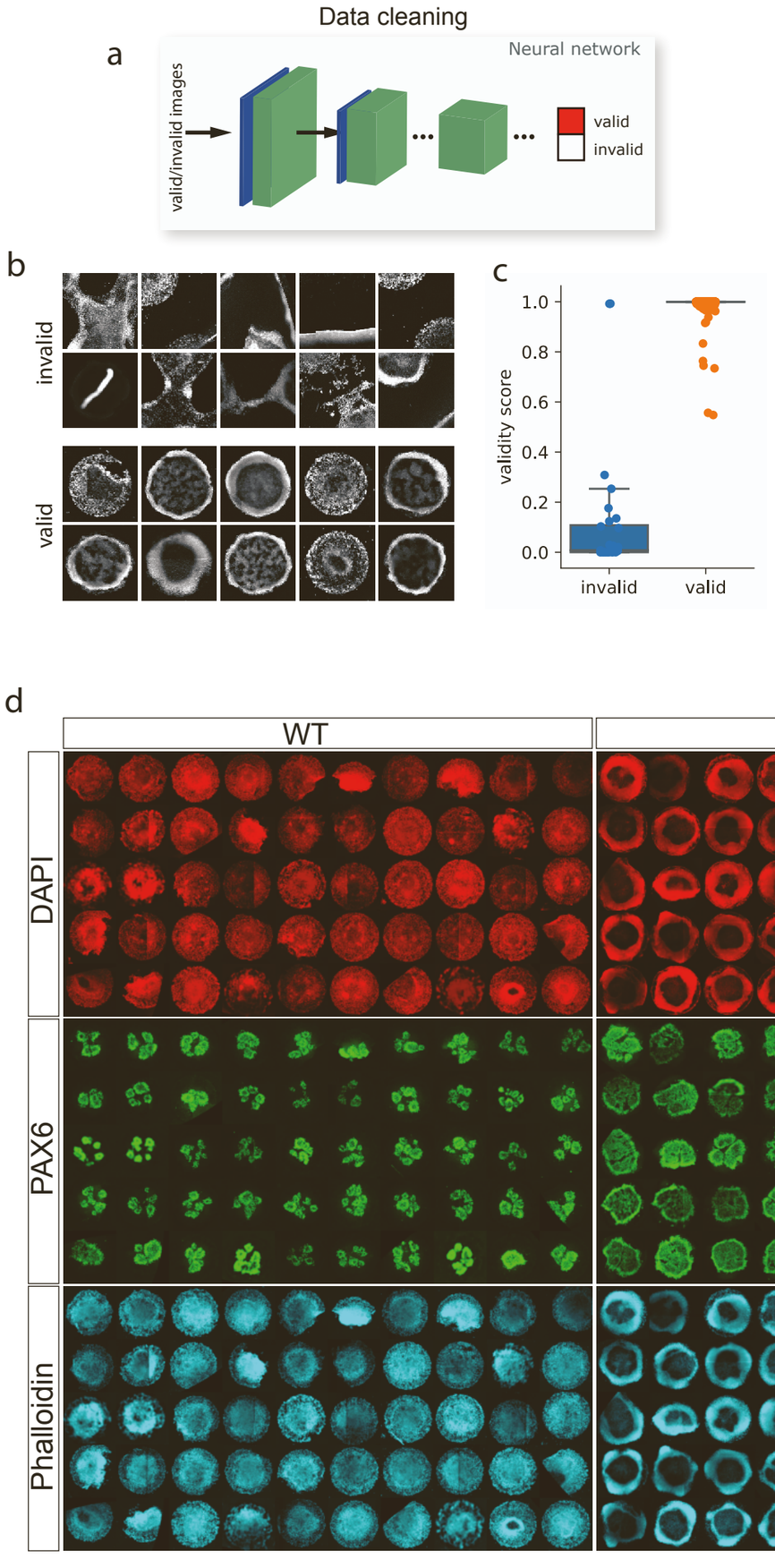

Fig. S1: **Data cleaning strategy, example images, details of comparison with other methods.** (a) Data cleaning approach using a neural network that is trained on valid and invalid organoids using their DAPI stains. (b) representative images from the two training sets. (c) Neural network can efficiently separate valid and invalid images. (d) Example images used in the training of the neural network in Fig. 1. (e) Illustration of the comparison of the neural network with other methods. PAX6 expression threshold is obtained using Otsu thresholding, then the number of pixels exceeding the threshold is summed. For UMAP quantification, the image is linearized and clustered using the python implementation of the UMAP algorithm. Confusion matrix, precision and recall is given for all methods.

Figure S2 related to Figure 2 & 3

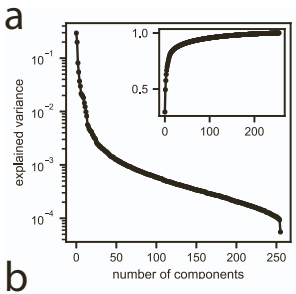

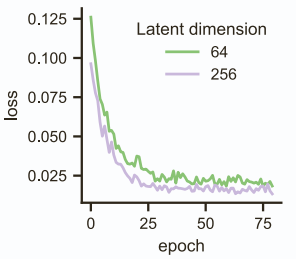

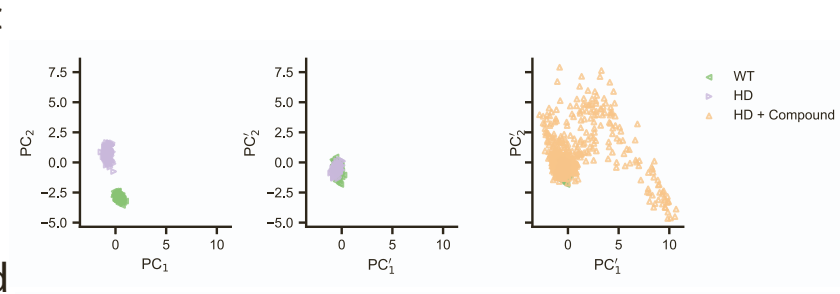

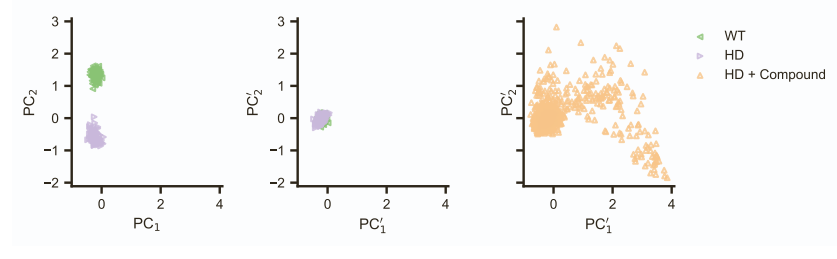

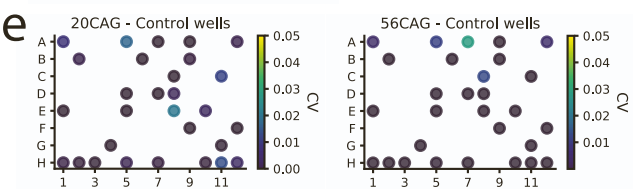

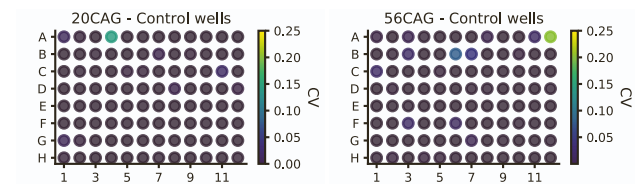

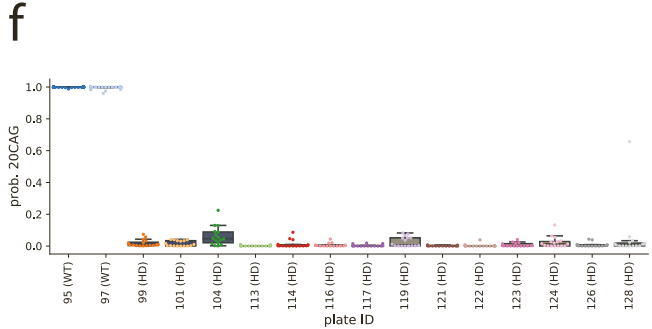

Fig. S2: **Details of autoencoder training and comparison of different latent space dimensions.** (a) Explained variance of the principal components of the latent vectors in Fig. 2d for a latent space with dimension 256. (b) Loss function for autoencoders with latent dimension 64 and 256. (c) Latent space before and after reduction of WT-HD direction, as in Fig. 2d, but for a 64-dimensional latent space. (d) Same as c, but for a 256-dimensional latent space. (e) CV values for per-well classification of randomly chosen 30% validation wells (top row) and CV values for organoids independent of wells (bottom row), related to Fig. 1e. (f) Per-plate variability for the classification results of control wells on the 14 plates presented in Fig. 3c.

Figure S3 related to Figure 4

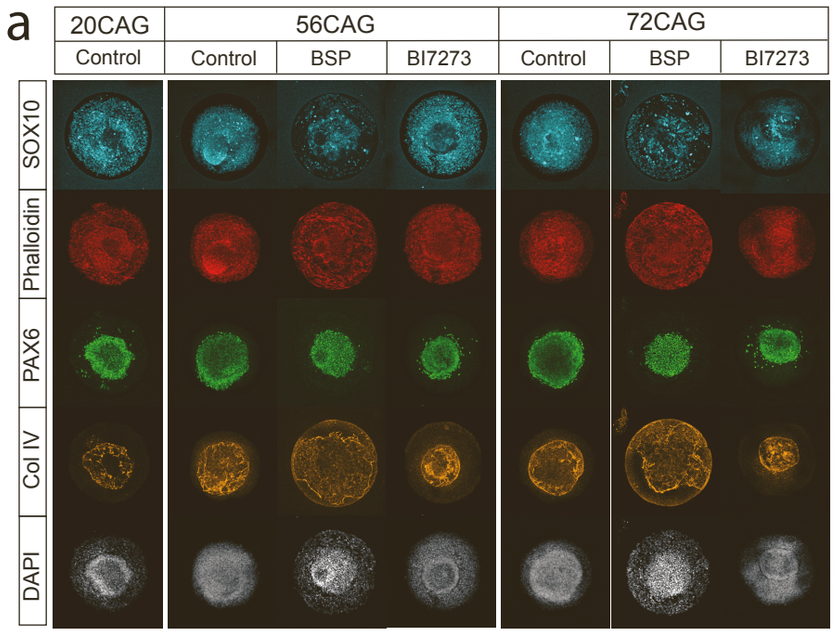

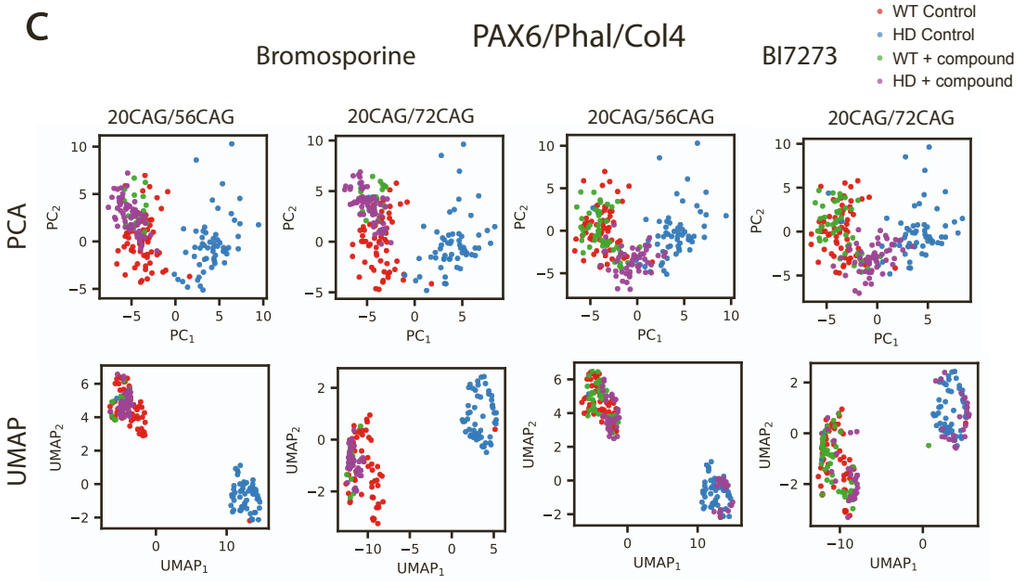

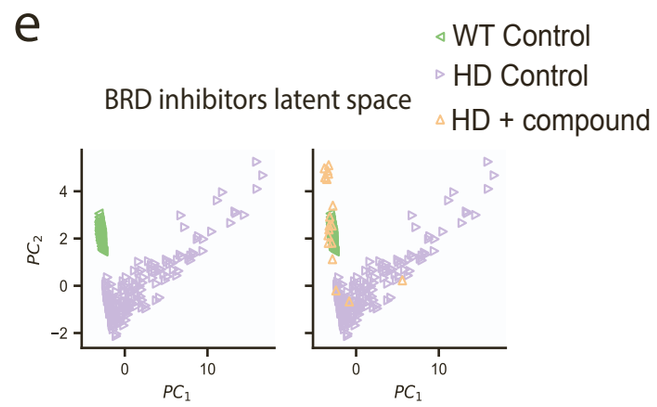

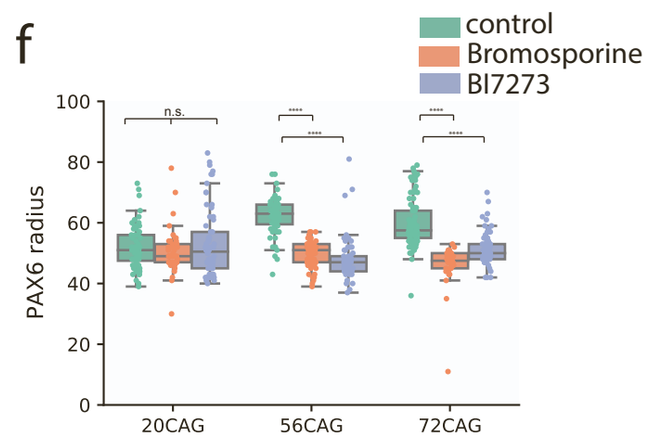

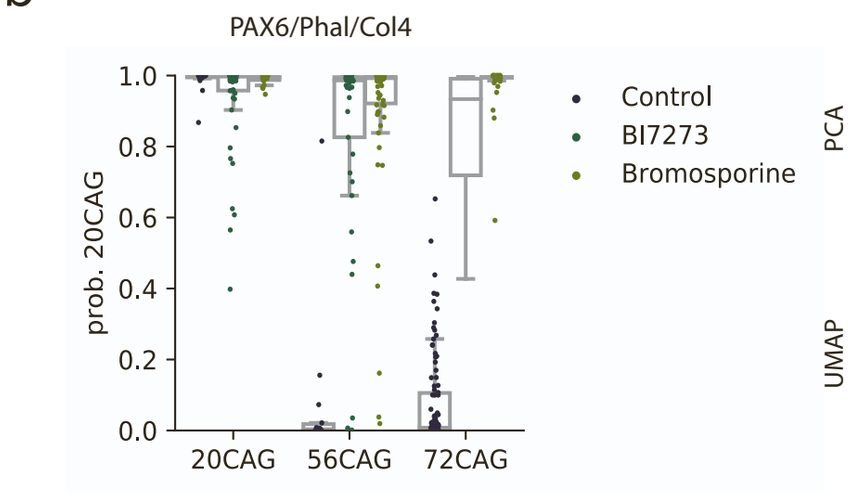

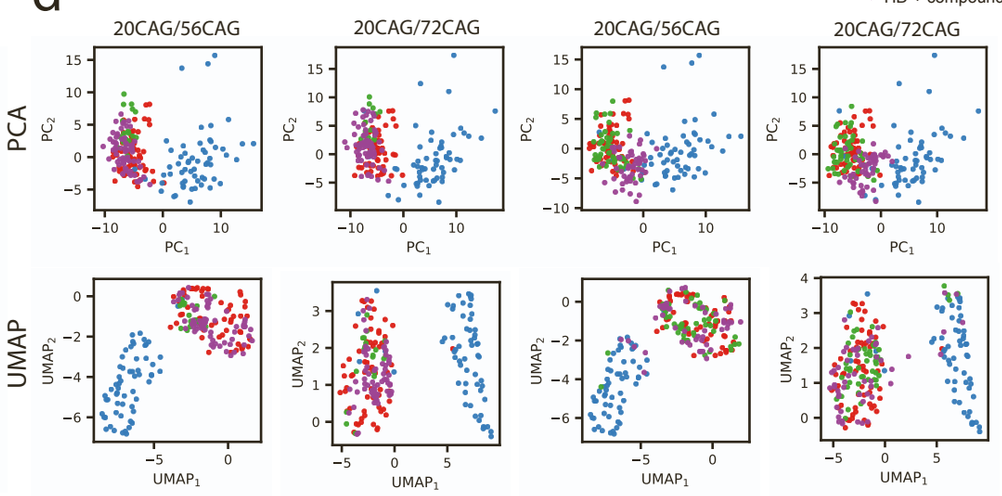

Fig. S3: **Comparison of 500 µm neuruloid experiment using different channels for autoencoder and classifier, with PCA and UMAP dimensionality reduction.** (a) representative colonies from three genotypes (WT-20CAG, HD-56CAG and HDD-72CAG) treated with DMSO control, Bromosporin (BSP), or BI7273. Latent space for PAX6/Phalloidin/Collagen IV channels. (b) Classification using PAX6/Phalloidin/Collagen IV channels. (c) PCA and UMAP clustering of the three genotypes treated of untreated with BI7273 using the three PAX6/Phalloidin/Collagen IV channels. (d) same using only the two PAX6/Phal channels. (e) Latent space for PAX6/Phalloidin channels. (f) Quantification of rescue using the PAX6 positive area. Clear rescue of the expanded PAX6 area for 56CAG and 72CAG cell lines can be observed. P-values: 20CAG Control, Bromosporine, BI7273: p = 0.783 (Kruskal-Wallace test for three samples). 56CAG Control-Bromosporine: p=7.6e-19 (Mann-Whitney U test), 56 Control-BI7273: p=1.01e-15 (Mann-Whitney), 72CAG Control-Bromosporine: p=1.19e-16 (Mann-Whitney), Control-BI7273: p=1.05e-14.

Figure S4 related to Figure 4

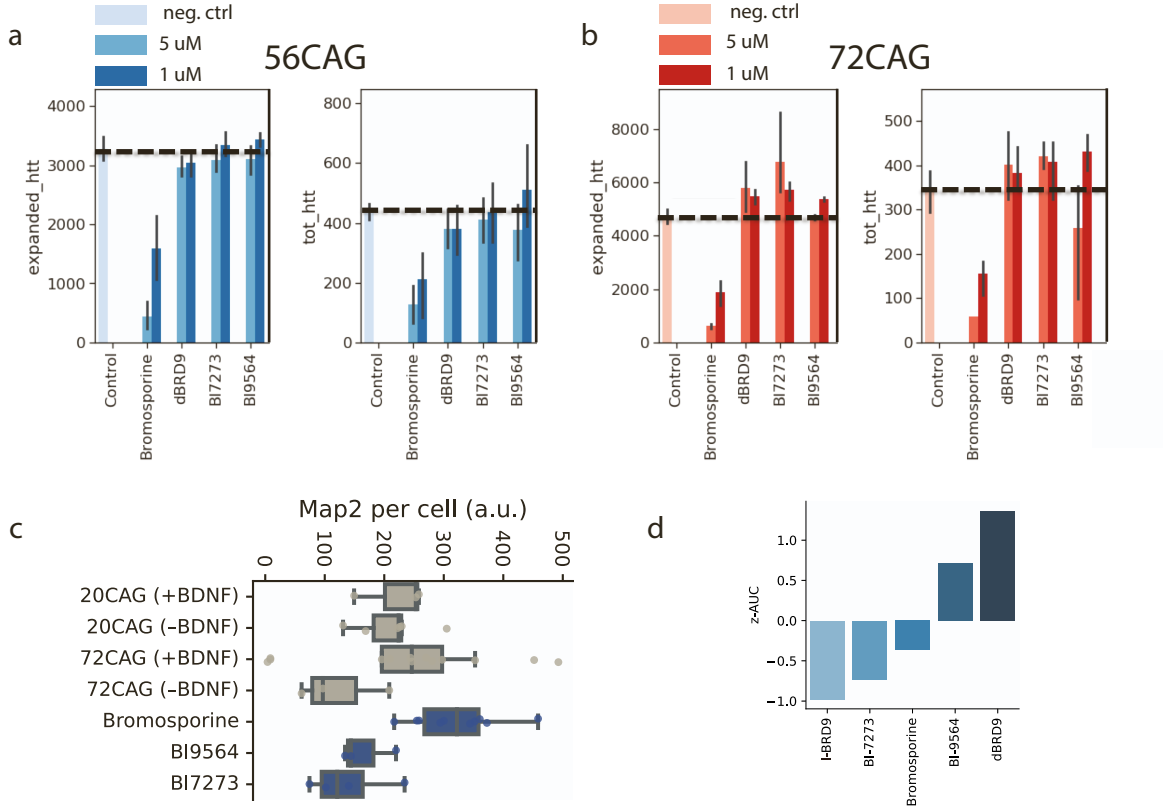

Fig. S4: **Htt lowering activity of bromodomain inhibitors.** Both total HTT levels and expanded HTT levels were measured in neuruloids by the MSD assay. Samples were treated for 7 days with DMSO control, 5 μM or 1 μM Bromosporine, BI7273, dBRD9 or BI9564. The assay was performed in two genetic backgrounds: 56CAG (a) and 72CAG (b). The dotted line on each graph refers to control levels of HTT in the DMSO treated control. (c) Quantification of MAP2 area per cell in the different conditions of the neuroprotection experiment from Fig. 4g-h. (d) z-AUC values associated with the dose-response curves in Fig 4b.